Effects of Alloying Elements M (M = Fe, Mo) on Phase Stability of $Cr_{23}C_6$ Carbides from First-principles

Yijie Yi[a], Weiwei Xu[b,*], Fangfang Xia[c], Tieqiang Gang[d], Lijie Chen[e,*]

School of Aerospace Engineering, Xiamen University, Xiamen 361005, China.

[a]yijie.yi@qq.com, [b]wwxu306@xmu.edu.cn, [c]65906715@qq.com,

[d]gangtq@xmu.edu.cn, [e]chenlijie@xmu.edu.cn

Keywords: Ni-based superalloys; First-principles calculations; $Cr_{23}C_6$ carbides; Phase stability

Abstract. The structural and electronic properties of $(Cr, M)_{23}C_6$ (M = Fe, Mo) with a full composition range of Cr/M ratio were carried out by first-principles calculations. The phase stability was investigated by calculating the reaction energy. Results reveal that $Cr_{22}FeC_6$, $Cr_{21}Fe_2C_6$, $Cr_{20}Fe_3C_6$, $Cr_{21}Mo_2C_6$ and $Cr_{20}Mo_3C_6$ are the stable phases. Alloying element Fe and Mo prefer to occupy the 4a and 8c sites of $Cr_{23}C_6$ carbides, respectively. Then the stabilized mechanism by alloying elements in $Cr_{23}C_6$ carbides was explored by employing the charge density difference. It provides the explanation that the high stability of $Cr_{22}FeC_6$ and $Cr_{21}Mo_2C_6$ is mainly attributed to the strengthening of covalent bonds between the 8c and 32f sites.

1. Introduction

Ni-based superalloys are widely used in hot section parts of aircraft engines because of their superior creep strength and thermo mechanical fatigue properties [1,2]. At high temperatures, owing to alternating stress, fatigue related failure becomes one of the primary failure modes for Ni-based superalloys in the hot section structures [3]. According to experimental observations, $M_{23}C_6$-type carbides are principle sites for fatigue crack initiations [4-6]. The previous study proposed that the precipitation of $M_{23}C_6$ carbides result in the formation of grain bound serrations [5]. It was also found by scanning electron microscopy that the fatigue cracks followed the continuous film of $M_{23}C_6$ carbides at the grain boundaries [6]. These facts indicate that $M_{23}C_6$ carbides have crucial effects on the formation of fatigue crack. Therefore, the information on the stability and structure of $M_{23}C_6$ carbides, as well as the corresponding mechanical and thermodynamic properties, is very helpful to deeply understand the mechanism of fatigue crack initiation.

Since the observation of γ-$M_{23}C_6$ carbides [7], the properties of γ-$M_{23}C_6$ binary phases had been systemically studied [8-21]. The structural, mechanical and electronic properties of $Cr_{23}C_6$ were reported by Jiang [10]. The phase stability of $M_{23}C_6$(M = V, Cr, Mn, Fe, Co, Ni) was discussed by Medvedeva [22]. However, $M_{23}C_6$-type carbides in multi-component alloys contain more than one metallic element. Generally, $Cr_{23}C_6$ can dissolve Fe, Mo, or W atoms and form complex γ-$(Cr, M)_{23}C_6$ phases [23]. Xie *et al.* [8,9] explored several compounds of γ-$(Cr, M)_{23}C_6$ (M = Fe, W, Ni) phases and found that Fe atoms preferred to substitute for Cr at 4a site and then 8c site of $Cr_{23}C_6$ phase. To simulate more substitution situations, Han *et al.* [24] studied γ-$Cr_{23}C_6$ compounds with each of the four metal Wyckoff sites being occupied in turns by Fe atoms. The obtained substitution sequence was 4a, 8c, 48h and 32f. Recently, the site preference of γ-$(Cr, M)_{23}C_6$ (M = Mo, W; x = 0-3) phases was investigated and $Cr_{21}M_2C_6$ (M = Mo, W) was found to be the most stable phase [23]. However, the affecting status of higher concentration of typical alloying elements in $Cr_{23}C_6$ carbides (e.g., Fe, Mo.) is still scarcely studied. Moreover, the alloying influence mechanism on the phase stability of $Cr_{23}C_6$ carbides is not fully understood as well.

In this work, we presented a comprehensive study for $(Cr, M)_{23}C_6$ (M = Fe, Mo) carbides with a full composition range of Cr/M ratio (*i.e.*, 0~1). The phase stability was investigated in terms of the formation and reaction energies. Then the charge density difference from electronic structure was adopted to further explore the influence mechanism of alloying elements on the phase stability. This work focuses on detailed theoretical analysis about the effects of doped Fe/Mo atoms on the phase

stability of $Cr_{23}C_6$ carbides in Ni-based superalloys for an in-depth understanding of the precipitation of $Cr_{23}C_6$-type carbides.

2. Details of Models and Calculations

All the calculations were performed by first-principles method based on the density functional theory [25-27]. For the exchange-correlation function, the generalized gradient approximation formulated by PBE [28] was used. To guarantee an accurate result, we employed a kinetic energy cut-off value of 500eV. The Brillouin zone sampling was set by the Monkhorst-Pack scheme [29] with a 13*13*13 k-point grid. The Methfessel-Paxton technique [30] for the reciprocal space integration was adopted for the structural relaxation with the smearing width of 0.10 eV, as recommended for highly accurate force and energy calculation in metals. Throughout the calculations, the convergence thresholds of total energy and the maximum force of ionic relaxation were set to 10^{-6} eV and 10^{-3} eV/Å, respectively.

$M_{23}C_6$-based multi-component carbides crystallize in the conventional cubic face-centered structure of the space group Fm-3m (*No.* 225) with four formula units. Each cell includes 92 metal atoms located at four types Wyckoff sites (*i.e.*, 4a, 8c, 32f and 48h) and 24 carbon atoms located at 24e Wyckoff site. Considering a wide range of Cr/M ratio, We constructs the calculated crystal structure with one or more Wyckoff sites being occupied by Fe or Mo. For example, in $Cr_{14}Fe_9C_6$, the Fe atoms occupy both the 4a and 32f sites. The detailed site occupation of doped Fe or Mo in $Cr_{23}C_6$ carbides with different Cr/M ratio will be given in the following sections.

3. Results and Discussions

3.1 Structural properties and Phase Stability

To evaluate the thermodynamic stability, we calculated the formation enthalpy (ΔH_f) per atom of carbides from the elements (α-Fe, bcc Cr and graphite). ΔH_f is defined as:

$$\Delta H_f\,(Cr_xM_yC_6) = [E(Cr_xM_yC_6) - x\cdot E(Cr) - y\cdot E(M) - 6\cdot E(C)]/(x+y+6). \quad (1)$$

At a pressure of 0 Pa and a temperature of 0 K, the ΔH_f is equal to the energy difference ΔE_f, namely, $\Delta H_f = \Delta E_f$. $E(Cr_xM_yC_6)$ is the total energy of carbides. E(Cr), E(M) and E(C) are the total energies of corresponding elements in their most stable state, respectively. Our calculated data of the related elements (Cr, *α*-Fe, Mo and Graphite) is presented in Table 1. Both the lattice constants and the total energy of elements agree well with the previous calculated data and experimental value in Refs. [18,24,31,32]. Note that the energy of graphite is calculated with consideration of the van der Waals interactions in graphite. As known, the formation energy (ΔH_f) can be used to evaluate the thermodynamic stability of materials. The negative ΔH_f means the stability of materials thermodynamically.

To characterize the phase stability of (Cr, M)$_{23}C_6$ (M = Fe, Mo) carbides, the reaction energy (ΔH_r) for a possible route relative to binary carbides (Cr_3C_2, Fe_3C and MoC) are introduced in the present study. In the Cr-rich part (R-Cr) with x≥20 in $Cr_xM_yC_6$ (M = Fe, Mo), iron and molybdenum exits as the form of Fe_3C and MoC carbides rather than elemental Fe and Mo, respectively. Thus, the formula reactions are $a\cdot Cr_3C_2 + b\cdot M_nC_m + c\cdot Cr \rightarrow d\cdot$ (Cr, M)$_{23}C_6$. In the M-rich part (R-M) with x≤3 in $Cr_xM_yC_6$, doped elements M exit as the form of elemental M and the reactions are $a\cdot Cr_3C_2 + b\cdot M_nC_m + c\cdot M \rightarrow d\cdot$(Cr, M)$_{23}C_6$. In the transition region (R-T) with 8≤x≤15 in $Cr_xM_yC_6$, doped elements M and chromium can both exist as form of elemental M and Cr and the reactions are $a\cdot Cr_3C_2 + b\cdot M_nC_m + c\cdot Cr + d\cdot M \rightarrow e\cdot$(Cr, M)$_{23}C_6$. To sum up, ΔH_r is described as:

$$\text{In R-Cr: } \Delta H_r\,(Cr_xM_yC_6) = d\cdot E_t\,(Cr_xM_yC_6) - a\cdot E_t\,(Cr_3C_2) - b\cdot E_t\,(M_nC_m) - c\cdot E_t\,(Cr), \quad (2)$$

$$\text{In R-M: } \Delta H_r\,(Cr_xM_yC_6) = d\cdot E_t\,(Cr_xM_yC_6) - a\cdot E_t\,(Cr_3C_2) - b\cdot E_t\,(M_nC_m) - c\cdot E_t\,(M), \quad (3)$$

$$\text{In R-T: } \Delta H_r\,(Cr_xM_yC_6) = e\cdot E_t\,(Cr_xM_yC_6) - a\cdot E_t\,(Cr_3C_2) - b\cdot E_t\,(M_nC_m) - c\cdot E_t\,(Cr) - d\cdot E_t\,(M), \quad (4)$$

where *a*, *b*, *c*, *d* and *e* are the ratio numbers of formula reactions. E_t ($Cr_xM_yC_6$), E_t (Cr_3C_2), E_t (M_nC_m) and E_t (X) represent the total energies of $Cr_xM_yC_6$, Cr_3C_2, M_nC_m phases and the pure metal X in their most stable states, respectively. The more negative ΔH_r implies more stable phase to be formed. Our calculated results of the relative binary carbides are presented in Table 1, together with available theoretical and experimental data [15,20,33-39]. Form Table 1, the lattice parameters and formation energies of relative binary carbides show a good agreement with other theoretical and experimental values in Refs. [15,20,33-39], indicating the reliability of this work.

TABLE 1. Calculated lattice parameters (*a*, *b*, and *c*), total energies E_{tot} and formation energies ΔH_f of elementary substance (Cr, Fe, Mo, and Graphite) and binary carbides (Cr_3C_2, Fe_3C, and MoC) in the ground state.

Phase	***a* [Å]**	***c* [Å]**	**E_{tot} [eV]**	**Phase**	***a* [Å]**	***b* [Å]**	***c* [Å]**	**E_{tot} [eV]**	**ΔE_f [eV/atom]**
Cr	2.865	-	-9.522	Cr_3C_2	5.475	2.789	11.462	-47.593	5.475
	2.833[a]		-9.521[a]		5.485[e]	2.789[e]	11.474[e]		5.485[e]
	2.866[b]				5.48[f]	2.79[f]	11.47[f]		5.48[f]
					5.54[g]	2.83[g]	11.49[g]		5.54[g]
α-Fe	2.831	-	-8.243	Fe_3C	5.035	6.717	4.483	-33.734	5.035
	2.83[c]		-8.309[a]		5.06[h]	6.70[i]	4.51[i]	-33.961[c]	5.06[h]
					5.08[j]	6.73[j]	4.52[j]		5.08[j]
Mo	3.164	-	-10.930	MoC	2.915	-	2.832	-20.406	2.915
	3.178[d]		-10.780[d]		2.909[k]		2.8487[k]		2.909[k]
					2.91[l]		2.83[l]		2.91[l]
					2.898[m]		2.809[m]		2.898[m]
Graphite	2.463	6.465	-9.344						
	2.464[b]	6.711[b]	-9.261[a]						

Note that the subscripts a-m represent the data from Refs. [24], [31], [18], [32], [15], [20] and [33-39], respectively.

The calculated lattice parameters, formation energies and reaction energies of $(Cr, M)_{23}C_6$ (M = Fe, Mo) carbides are listed in Table 2. The calculated lattice parameters and formation energies show little deviations from others calculated results [18,23,24] and experimental data [7,40,41]. The most negative reaction energy is found for $Cr_{22}FeC_6$ and $Cr_{21}Mo_2C_6$ among $(Cr, Fe)_{23}C_6$ and $(Cr, Mo)_{23}C_6$ carbides, which indicates the maximum exothermic reaction of formation from its relative elemental constituents.

According to the reaction energies from Table 2, the negative reaction energies are found for $Cr_{22}FeC_6$, $Cr_{21}Fe_2C_6$, and $Cr_{20}Fe_3C_6$, which indicates that these phases are stable. Hence, the stable phases are concentrated in the Cr-rich part. This result differs from prediction from Han [24] whose calculated formation energies indicate that there are also several other stable phases in the transition region with higher Fe content. This is mainly because of different calculation methods of enthalpy for graphite. The energy of graphite in this work is calculated considering van der Waals interactions in graphite rather than performing calculations for diamond carbon and then subtracting the energy difference between diamond and graphite [18]. Based on the accurate energy calculation of graphite, the enthalpy of graphite obtained from this work is more negative than that from Han *et al.* [24]. Therefore our calculations reveals that $(Cr, Fe)_{23}C_6$ phases exhibit a narrow range of formation at the ground state, which is more reasonable and agrees well with the experimental reports [42,43]. $Cr_{22}FeC_6$ is the most stable carbide with the reaction energy of -8.265 eV. The previous study also noted that $Cr_{22}FeC_6$ was more stable than other substitution situations with Fe [44].

On the other hand, in $(Cr, Mo)_{23}C_6$ carbides, $Cr_{21}Mo_2C_6$ and $Cr_{20}Mo_3C_6$ are the stable phases due to their negative ΔH_f values. According to the calculated ΔH_r values, it's indicated that $Cr_{21}Mo_2C_6$ with the 8c site being fully occupied by Mo atoms is the most stable phase. It means that the 8c is the preferential site for doped Mo in $Cr_{23}C_6$ structure, which is identical with the report from Lv [23]. Interestingly, for $Cr_{22}MoC_6$, the formation energy ΔH_f is negative, illustrating its thermodynamic stability, while the reaction energy shows its phase instability. The previous investigation also stated that Mo atom had little probability to occupy 4a site of $Cr_{23}C_6$ structure [9].

In terms of reaction energy, the order of phase stability can be evaluated. Han *et al*. [24] suggested that the stability of (Cr, Fe)$_{23}$C$_6$ phases follows the sequence of $Cr_{22}FeC_6 \geq Cr_{21}Fe_2C_6 \geq Cr_{11}Fe_{12}C_6 \geq Cr_{15}Fe_8C_6$, by comparing the reaction energies. According to the data shown in Table 2, our works reproduce Han's results. The obtained reaction energies of $Cr_{22}FeC_6$, $Cr_{21}Fe_2C_6$, $Cr_{20}Fe_3C_6$, $Cr_{15}Fe_8C_6$ and $Cr_{11}Fe_{12}C_6$ are -8.265 eV, -0.562 eV, -1.705 eV, 0.506 eV and 0.122 eV, respectively. Thus, the doped Fe atoms in $Cr_{23}C_6$ phase will preferentially occupy Cr atoms in the 4a site and then 8c, after which Fe atoms occupy both 4a and 8c, 48h and 32f with the increase of Fe contents. For (Cr, Mo)$_{23}$C$_6$ carbides, however, the calculation results show that the preferential sites for the doped Mo in $Cr_{23}C_6$ structure is 8c. This means the doped Fe and Mo atoms have different effects on the stability of $Cr_{23}C_6$ carbides.

TABLE 2. Calculated lattice constants a, formation energies ΔH_f and reaction energies ΔH_r of (Cr, M)$_{23}$C$_6$ (M = Fe, Mo).

Carbides	Site Occupation	a [Å]	ΔH_f [eV/atom]	ΔH_r [eV]	Carbides	Site Occupation	a [Å]	ΔH_f [eV/atom]	ΔH_r [eV]
$Cr_{23}C_6$	Cr: 4a, 8c, 32f, 48h	10.542 10.659[a]	-0.058 -0.071[a] -0.078[c]	-0.651					
$Cr_{22}FeC_6$	Fe: 4a Cr: 8c, 32f, 48h	10.529 10.516[b]	-0.076 -0.089[b]	-8.265	$Cr_{22}MoC_6$	Mo: 4a Cr: 8c, 32f, 48h	10.589 10.651[f]	-0.030 -0.078[f]	0.205
$Cr_{21}Fe_2C_6$	Fe: 8c Cr: 4a, 32f, 48h	10.517 10.507[b]	-0.029 -0.050[b]	-0.562	$Cr_{21}Mo_2C_6$	Mo: 8c Cr: 4a, 32f, 48h	10.628 10.686[f]	-0.072 -0.123[f]	-1.163
$Cr_{20}Fe_3C_6$	Fe: 4a, 8c Cr: 32f, 48h	10.505	-0.047	-1.705	$Cr_{20}Mo_3C_6$	Mo: 4a, 8c Cr: 32f, 48h	10.671 10.728[f]	-0.048 -0.103[f]	-1.025
$Cr_{15}Fe_8C_6$	Fe: 32f Cr: 4a, 8c, 48h	10.412 10.402[b]	0.017 -0.0005[b]	0.506	$Cr_{15}Mo_8C_6$	Mo: 32f Cr: 4a, 8c, 48h	10.982	0.081	3.289
$Cr_{14}Fe_9C_6$	Fe: 4a, 32f Cr: 8c, 48h	10.410	0.004	0.133	$Cr_{14}Mo_9C_6$	Mo: 4a, 32f Cr: 8c, 48h	11.018	0.101	3.899
$Cr_{13}Fe_{10}C_6$	Fe: 8c, 32f Cr: 4a, 48h	10.421	0.054	1.581	$Cr_{13}Mo_{10}C_6$	Mo: 8c, 32f Cr: 4a, 48h	11.074	0.076	3.151
$Cr_{12}Fe_{11}C_6$	Fe: 4a, 8c, 32f Cr: 48h	10.444	0.039	1.141	$Cr_{12}Mo_{11}C_6$	Mo: 4a, 8c, 32f Cr: 48h	11.107	0.091	3.606
$Cr_{11}Fe_{12}C_6$	Fe: 48h Cr: 4a, 8c, 32f	10.465 10.461[b]	0.004 -0.018[b]	0.122	$Cr_{11}Mo_{12}C_6$	Mo: 48h Cr: 4a, 8c, 32f	11.155	0.060	2.699
$Cr_{10}Fe_{13}C_6$	Fe: 4a, 48h Cr: 8c, 32f	10.471	0.017	0.511	$Cr_{10}Mo_{13}C_6$	Mo: 4a, 48h Cr: 8c, 32f	11.200	0.084	3.384
$Cr_9Fe_{14}C_6$	Fe: 8c, 48h Cr: 4a, 32f	10.466	0.012	0.377	$Cr_9Mo_{14}C_6$	Mo: 8c, 48h Cr: 4a, 32f	11.212	0.010	0.043
$Cr_8Fe_{15}C_6$	Fe: 4a, 8c, 48h Cr: 32f	10.457	0.017	0.513	$Cr_8Mo_{15}C_6$	Mo: 4a, 8c, 48h Cr: 32f	11.255	0.032	1.867
$Cr_3Fe_{20}C_6$	Fe: 32f, 48h Cr: 4a, 8c	10.411	0.057	0.660	$Cr_3Mo_{20}C_6$	Mo: 32f, 48h Cr: 4a, 8c	11.518	0.090	3.489
$Cr_2Fe_{21}C_6$	Fe: 4a, 32f, 48h Cr: 8c	10.422	0.060	1.167	$Cr_2Mo_{21}C_6$	Mo: 4a, 32f, 48h Cr: 8c	11.552	0.109	12.012
$CrFe_{22}C_6$	Fe: 8c, 32f, 48h Cr:4a	10.448	0.068	0.847	$CrMo_{22}C_6$	Mo: 8c, 32f, 48h Cr:4a	11.573	0.043	6.229
$Fe_{23}C_6$	Fe: 4a, 8c, 32f, 48h	10.474 10.467[d] 10.639[e]	0.085 0.019[d] 0.036[e]	0.436	$Mo_{23}C_6$	Mo: 4a, 8c, 32f, 48h	11.609	0.057	2.480

Note that the subscripts a, c, e represent the experimental data from Refs. [7], [40], [41], and the subscripts b, d, f represent the theoretical data from Refs. [24], [18], [23].

3.2 Charge Density Difference Analysis

The advantage of first-principles calculation is its ability to reveal the electronic origin of the calculated macroscopic properties. To further explore the stabilized mechanism by alloying elements in $Cr_{23}C_6$ carbides, the electronic structures and chemical bonding characteristics of (Cr, M)$_{23}$C$_6$ (M = Fe, Mo) carbides were discussed via charge density difference maps (CDD). Figs. 1 and 2 represent the CDD maps of $Cr_{23}C_6$, $Cr_{22}FeC_6$, $Cr_{15}Fe_8C_6$, $Cr_{22}MoC_6$ and $Cr_{21}Mo_2C_6$ on the (1-10) crystal plane, respectively. It can be seen that electrons concentrate on the C atoms at the 24e

site in $Cr_{23}C_6$ phase. Electrons in the red color area between Cr atoms at 32f site and C atoms are effectively localized, indicating the strong covalent interactions. In the dark red area with dense contour lines between Cr atoms at 32f site and Cr atoms at 8c site, more powerful covalent bonds form. In addition, interactions between Cr atoms at 32f site are in orange color and distributed through the matrix map, which indicates the characteristics of metallic bonding. It is observed that the bonding behavior of $(Cr, M)_{23}C_6$ (M = Fe, Mo) compounds are a mix of metallic and covalent characters.

In a comparison of Fig. 1(b) with Fig. 1(a), the bonds between 4a site and 48h site almost remain as they were when Fe atoms enter the $Cr_{23}C_6$ structure and form $Cr_{22}FeC_6$. However, the light orange area between 32f site and the deep red area with denser contour lines between 8c site and 32f site reveal that part of electrons between Cr atoms at 32f site transfer to the area of the bonds between 8c site and 32f site. This leads to the weakened metallic bonding between Cr atoms at 32f site and strengthen the covalent bonds between Cr atoms at 32f site and Cr atoms at 8c site. It is generally agreed that the covalent bond is more stable than the metallic bond. Thus, $Cr_{22}FeC_6$ possesses higher stability according to CDD analysis, which is identical with the result by calculating formation and reaction energies. In contrast, Fig. 1(c) shows that part of electrons between 8c site and 32f site transfer to the area of the bonds between Cr atoms at 32f site, indicating that the covalent bonds between 8c site and 32f site are weakened in the $Cr_{15}Fe_8C_6$ phase. Hence, $Cr_{15}Fe_8C_6$ is less stable than $Cr_{23}C_6$ and $Cr_{22}FeC_6$. Similarly, it is apparent from Fig. 2 that the covalent bonds between 8c site and 32f site in $Cr_{21}Mo_2C_6$ are more strong than those in $Cr_{22}Mo_1C_6$, which reveals the higher stability of $Cr_{21}Mo_2C_6$. By analyzing the CDD maps, we find that Fe/Mo atoms in the preferential sites will strengthen the covalent bonds between 8c site and 32f site in $Cr_{23}C_6$ carbides and form the stable compounds consequently.

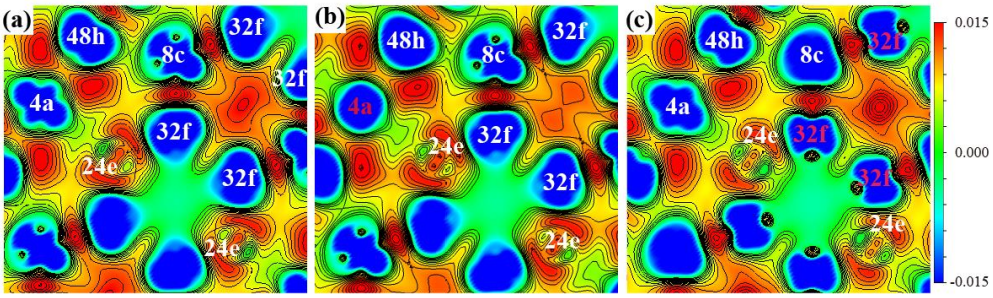

FIGURE 1. Contour plots of charge density differences (CDD) on the (1-10) plane from -0.015 (blue) to 0.015 (red) electrons·Å^{-3} for $(Cr, Fe)_{23}C_6$ carbides: (a) pure $Cr_{23}C_6$, (b) $Cr_{22}Fe_1C_6$, and (c) $Cr_{15}Fe_8C_6$ carbides. Note that the red and blue indicates regions of high electron localization and delocalization.

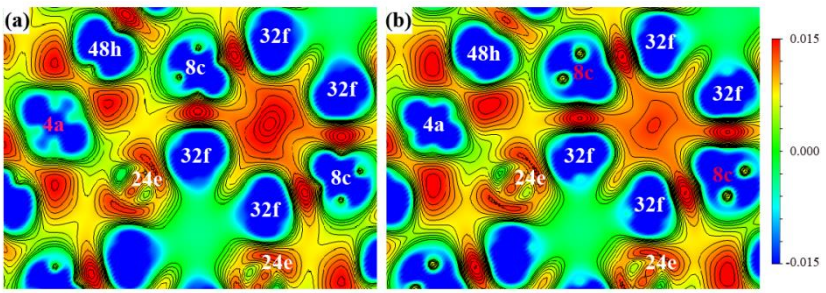

FIGURE 2. Contour plots of charge density differences (CDD) on the (1-10) plane from -0.015 (blue) to 0.015 (red) electrons·Å^{-3} for $(Cr, Mo)_{23}C_6$ carbides: (a) $Cr_{22}Mo_1C_6$ and (b) $Cr_{21}Mo_2C_6$. Note that the red and blue indicates regions of high electron localization and delocalization.

4. Summary

The structure, stability and electronic property of $(Cr, M)_{23}C_6$ (M = Fe, Mo) carbides with a full composition range of Cr/Fe and Cr/Mo ratios are investigated by using the first-principles calculations. The main conclusions from this work can be drawn as follows:

(1) The calculated lattice constants and energies for $(Cr, M)_{23}C_6$ (M = Fe, Mo) carbides, as well as relative elements and binary carbides, coincide well with the available data, which indicates the reliability of this work.

(2) For $(Cr, Fe)_{23}C_6$, the stable phases are $Cr_{22}FeC_6$, $Cr_{21}Fe_2C_6$, and $Cr_{20}Fe_3C_6$. For $(Cr, Mo)_{23}C_6$, the stable phases are $Cr_{21}Mo_2C_6$ and $Cr_{20}Mo_3C_6$. It is revealed that the stable phases for $(Cr, M)_{23}C_6$ (M = Fe, Mo) carbides are concentrated in the Cr-rich part, while high concentration of alloying elements decrease the stability of $Cr_{23}C_6$.

(3) Theoretically, doped Fe atoms preferentially substitute Cr atoms in the 4a site and then 8c site of $Cr_{23}C_6$ structure, after which, Fe atoms occupy both 4a and 8c, 48h and 32f sites with the increase of Fe contents. Mo atoms will substitute Cr atoms in the 8c site firstly and then 4a site.

(4) Doped Fe atoms at 4a site or doped Mo atoms at 8c site of $Cr_{23}C_6$ structure strengthen the covalent bonds between the metal atoms at 8c site and 32f site, which contributes to the high stability of $Cr_{22}FeC_6$ and $Cr_{21}Mo_2C_6$.

Acknowledgements

Lijie Chen acknowledges support from the National Natural Science Foundation of China under Grant No. 51475396. Weiwei Xu acknowledges support from the National Natural Science Foundation of China under Grant No. 51601161.

References

[1] CT Sims, NS Stoloff, and WC Hagel, eds. *Superalloys II: High Temperature Materials for Aerospace and Industrial Power*, A Wiley-Interscience Publication, John Wiley and Sons Inc., New York, NY (1987): 97-133.
[2] Q. Feng, T. Nandy, S. Tin and T. Pollock, Acta Materialia 51 (1), 269-284 (2003).
[3] J. King, Materials science and technology 3 (9), 750-764 (1987).
[4] F. Alexandre, S. Deyber and A. Pineau, Scripta Materialia 50 (1), 25-30 (2004).
[5] L. Jiang, R. Hu, H. Kou, J. Li, G. Bai and H. Fu, Materials Science and Engineering: A 536, 37-44 (2012).
[6] A. Malekbarmi, S. Zangeneh and A. Roshani, Engineering Failure Analysis 18 (5), 1262-1271 (2011).
[7] A. Westgren, Nature 132, 480 (1933).
[8] J. Xie, N. Chen, J. Shen, L. Teng and S. Seetharaman, Acta materialia 53 (9), 2727-2732 (2005).
[9] J. Xie, J. Shen, N. Chen and S. Seetharaman, Acta materialia 54 (18), 4653-4658 (2006).
[10] C. Jiang, Applied Physics Letters 92 (4), 1909 (2008).
[11] M. Widom and M. Mihalkovic, Journal of materials research 20 (01), 237-242 (2005).
[12] P. Ohodnicki Jr, N. Cates, D. Laughlin, M. McHenry and M. Widom, Physical Review B 78 (14), 144414 (2008).
[13] J. Wallenius, N. Sandberg and K. Henriksson, Journal of Nuclear Materials 415 (3), 316-319 (2011).
[14] A. V. dos Santos, Physica B: Condensed Matter 387 (1), 136-142 (2007).
[15] Y. Li, Y. Gao, B. Xiao, T. Min, Y. Yang, S. Ma and D. Yi, Journal of Alloys and Compounds 509 (17), 5242-5249 (2011).
[16] H. Faraoun, Y. Zhang, C. Esling and H. Aourag, Journal of applied physics 99 (9), 093508 (2006).
[17] J. Häglund, A. F. Guillermet, G. Grimvall and M. Körling, Physical Review B 48 (16), 11685 (1993).
[18] C. Fang, M. Van Huis, M. Sluiter and H. Zandbergen, Acta Materialia 58 (8), 2968-2977 (2010).

[19] C. Fang, M. Sluiter, M. Van Huis, C. Ande and H. Zandbergen, Physical review letters 105 (5), 055503 (2010).
[20] C. Fang, M. Van Huis and H. Zandbergen, Physical Review B 80 (22), 224108 (2009).
[21] C. Fang, M. Van Huis and H. Zandbergen, Scripta Materialia 63 (4), 418-421 (2010).
[22] N. Medvedeva, D. Van Aken and J. Medvedeva, Computational Materials Science 96, 159-164 (2015).
[23] Z. Lv, F. Dong, Z. Zhou, G. Jin, S. Sun and W. Fu, Journal of Alloys and Compounds 607, 207-214 (2014).
[24] J. Han, C. Wang, X. Liu, Y. Wang and Z.-K. Liu, Journal of Physics: Condensed Matter 24 (50), 505503 (2012).
[25] G. Kresse and J. Hafner, Physical Review B 48 (17), 13115 (1993).
[26] G. Kresse and J. Hafner, Physical Review B 49 (20), 14251 (1994).
[27] G. Kresse and J. Furthmüller, Computational Materials Science 6 (1), 15-50 (1996).
[28] J. P. Perdew, K. Burke and M. Ernzerhof, Physical review letters 77 (18), 3865 (1996).
[29] H. J. Monkhorst and J. D. Pack, Physical review B 13 (12), 5188 (1976).
[30] M. Methfessel and A. Paxton, Physical Review B 40 (6), 3616 (1989).
[31] Dinsdale A T. SGTE unary database, version 4.4. 2002.
[32] Y. Wang, S. Curtarolo, C. Jiang, R. Arroyave, T. Wang, G. Ceder, L.-Q. Chen and Z.-K. Liu, Calphad 28 (1), 79-90 (2004).
[33] J. Glaser, R. Schmitt and H. Meyer, ChemInform 34 (52) (2003).
[34] S. Meschel and O. Kleppa, Journal of alloys and compounds 257 (1), 227-233 (1997).
[35] I. Shein, N. Medvedeva and A. Ivanovskii, Physica B: Condensed Matter 371 (1), 126-132 (2006).
[36] I. Wood, L. Vočadlo, K. Knight, D. P. Dobson, W. Marshall, G. D. Price and J. Brodholt, Journal of Applied Crystallography 37 (1), 82-90 (2004).
[37] M. Kavitha, G. S. Priyanga, R. Rajeswarapalanichamy and K. Iyakutti, Materials Chemistry and Physics 169, 71-81 (2016).
[38] Y. Liu, Y. Jiang, J. Feng and R. Zhou, Physica B: Condensed Matter 419, 45-50 (2013).
[39] E. Clougherty, K. Lothrop and J. Kafalas, Nature 191, 1194 (1961).
[40] Carnegie Mellon Alloy Database. Information on http://alloy.phys.cmu.edu/
[41] A. F. Guillermet and G. Grimvall, Journal of Physics and Chemistry of Solids 53 (1), 105-125 (1992).
[42] V. Raghavan, Journal of Phase Equilibria(USA) 23 (6), 513-514 (2002).
[43] S. Atamert and H. Bhadeshia, Materials Science and Engineering: A 130 (1), 101-111 (1990).
[44] K. O. Henriksson, N. Sandberg and J. Wallenius, Applied Physics Letters 93 (19), 191912 (2008).